Controllable Structure, Properties, and Degradation of the Electrospun PLGA/PLA-Blended Nanofibrous Scaffolds

Hua Liu,[1,2] Shudong Wang,[1,2] Ning Qi[3]

[1]*Department of Textile Engineering, College of Yancheng Textile Vocational Technology, Yancheng 224005, China*
[2]*Jiangsu R&D Center of the Ecological Textile Engineering &Technology, Yancheng College of Textile Technology, Yancheng 224005, China*
[3]*College of Textile and Clothing Engineering, Soochow University, Suzhou 215021, China*

Received 25 August 2011; accepted 6 January 2012
DOI 10.1002/app.36757
Published online in Wiley Online Library (wileyonlinelibrary.com).

ABSTRACT: In this research, the PLGA/PLA-blended nanofibers were successfully prepared by electrospinning. The macro–micro structure, thermal stability, hydrophilicity, mechanical properties, and *in vitro* degradation of the electrospun PLGA/PLA nanofibrous scaffolds are characterized by means of SEM, FTIR, DSC, TG, contact angle, instron tensile tester, and degradation testing. The results showed that electrospun PLGA/PLA-blended nanofibrous scaffolds possessed nanofibrous and porous structures. The structural stability, crystallinity, wettability, and mechanical properties, especially the *in vitro* degradation rate, of the electrospun PLGA/PLA-blended nanofibrous scaffolds could be controlled by regulating the blended ratio of the poly(lactide-*co*-glycolide) (PLGA) and poly(lactide) (PLA). The results indicated that the electrospun PLGA/PLA-blended nanofibrous scaffolds could be considered as ideal candidates for tissue engineering scaffolds. © 2012 Wiley Periodicals, Inc. J Appl Polym Sci 000: 000–000, 2012

Key words: electrospinning; PLGA; PLA; controllable properties; degradation

INTRODUCTION

Electrospinning has been paid much attention to because it can prepare three-dimensional nano-scale fibrous membranous or tubular scaffolds with an extremely large surface-to-volume and high porosity. Moreover, the composition and structure can be controlled to achieve desired properties and functionality. Electrospinning has been applied widely in biomedical areas, such as nerve guidance conduit, wound dressing, bone regeneration, and vascular graft. Presently, a large number of reports and studies have been issued emphasizing on the electrospun natural and synthetic polymers used for biomaterials.[1–5] Many studies demonstrate that cell attachment, spreading, and proliferation were enhanced greatly on these nanofibrous structures.

The composition of the original material has a great influence on the morphological, mechanical, biodegradable, and biological properties of the electrospun scaffold. Among the natural and synthetic polymers, poly(lactide) (PLA) and poly(lactide-*co*-glycolide) (PLGA) are preferred when compared to natural polymers because they enable control on the rate of degradation, provide high mechanical strength, and are biocompatible.[6,7] PLA is a biocompatible and biodegradable synthetic polymer. Most importantly, PLA has a higher breaking strength and initial modulus when compared to the PLGA.[8] However, PLA with poor hydrophilic properties are well-known for lacking bioactivity and cell affinity, and the degradation rate of PLA is relatively slow.[9] PLGA, the random copolymer of lactic acid (LA) and glycolic acid (GA), has been widely used for tissue engineering applications. Many researchers have recently investigated PLGA as one of the candidate materials for biomedical applications because it is well known for its good biocompatibility, good degradation behavior, good oxygen and water vapor permeability, and minimal inflammatory reaction.[10–12] However, the greater degradation rate and lower breaking strength (compare to PLA) of PLGA restrict the extensive applications.[13]

In this research, we fabricate the scaffolds with controllable structure, mechanical properties, and degradation rate by regulating the component of PLA and PLGA via electrospinning. Presently, a number of studies have been made to concentrate on the electrospun PLA and PLGA nanofibrous scaffolds. However, there are few reports about the

Correspondence to: S. Wang (sdwang1983@163.com).
Contract grant sponsor: Chinese Jiangsu Province Key Lab Foundation; contract grant number: KJS0817.
Contract grant sponsor: Cooperative innovation in the trinity of enterprises, campuses and research institutes in Jiangsu Province, China; contract grant number: BY2010129.

© 2012 Wiley Periodicals, Inc.

PLGA/PLA-blended nanofiber and its degradation. In this article, the PLGA/PLA-blended nanofibrous scaffolds are prepared by electrospinning. The structure, microstructure, thermal stability, wettability, mechanical properties, and degradation of the electrospun PLGA/PLA nanofibrous scaffolds are characterized by means of scanning electron microscope (SEM), Fourier transform-infrared (FTIR), differential scanning calorimetry (DSC), thermogravimetric analysis (TG), contact angle (CA), instron tensile tester, and degradation testing.

EXPERIMENT

Materials

PLGA (LA : GA = 75 : 25) with molecular weight 1.1×10^5 and PLA with molecular weight 1.0×10^5 were purchased from Natureworks Co., Minnetonka, MN. Chloroform, acetone (solvents used for electrospinning), and all the other reagents were obtained from Shanghai Chemistry Reagent Co., Shanghai, China. All the reagents were of analytical grade.

Preparation of the electrospun PLGA/PLA-blended nanofibers

PLGA was blended with PLA in different ratios (100 : 0, 70 : 30, 50 : 50, and 0 : 100 w/w). Both of them were dissolved in a mixed solvent of chloroform and acetone (2 : 1 volume ratio) to obtain spinning solution with 5 wt % concentrations. For electrospinning,[14] a high electric potential was applied to a droplet of solution at the tip (inner diameter = 0.9 mm) of a syringe needle in a horizontal mount. The electrospun PLGA/PLA-blended nanofibers were collected on the collector with a cathode. The spinning conditions were set as follows (listed in the order of voltage, polar distance, and flow rate): 25 kV, 15 cm, and 0.1 mL/h.

Viscosity of the spinning solution

The viscosities of the uniform PLGA/PLA-blended spinning solution with different blended ratios were measured by a rheometer tester (ADVANCED RHEOMETER, AR2000, USA) under different shear rates.

Morphological characterization

The morphology of the electrospun PLGA/PLA nanofibers was observed by a JSM SEM (JEOL Co., Japan) with the magnification of 10,000. Based on the SEM images, fiber diameter and standard deviation were analyzed with an image analysis program (Adobe Photoshop 7.0). Utilizing SEM images, the surface area of the pores were calculated and then normalized to a circular area. The circular diameter was regarded as the pore diameter, using three samples in each group. The porosity of the PLGA/PLA-blended scaffold was calculated according to the method described by Vaz et al.[15] Briefly, the porosity (ε) was calculated with the measured bulk density of the samples and the standard density of PLGA/PLA (casting film from the spinning solution), as shown in eq. (1).

$$\varepsilon\,(\%) = \left(1 - \frac{\rho}{\rho_0}\right) \times 100 \tag{1}$$

ρ stands for the bulk density and ρ_0 stands for standard density.

Composition and thermal stability

The composition and thermal stability of the PLGA/PLA-blended nanofibrous scaffolds were measured by FTIR spectra and TG-DSC, respectively. The FTIR spectrum was obtained by using a series spectrometer (Nicolet 5700, USA) in the spectral region of 4000–400 cm^{-1}. TG-DSC curves were obtained by a thermal analysis instrument (Diamond 5700, PE Co., USA) at a heating rate of 10°C/min, a scan range of 40–400°C, and a nitrogen gas flow rate of 120 mL/min.

Wettability of the PLGA/PLA-blended nanofibrous scaffolds

The wettability of the PLGA/PLA-blended nanofibrous scaffolds was characterized by water uptake and CA of a water droplet on the surface. The PLGA/PLA-blended nanofibrous scaffolds were immersed into warm de-ionized water (37°C; 1 : 100 mass ratio) for 30 min, and the scaffolds were put on the filter screen for 5 min. Then, the mass before and after immersion was measured by an analytical balance (Atartorius BS224S, Sartorius Co., Germany). And the water uptake was calculated with eq. (2). The CAs of the electrospun PLGA/PLA-blended nanofibrous scaffolds were measured with a drop shape analysis system (SZ10-JC2000A, Shanghai Zhongchen digital technique Co., China) in the sessile mode at room temperature (25°C). Three samples of each material type were tested.

$$\textit{Water uptake}\ (\%) = \frac{m_1 - m_0}{m_0} \times 100 \tag{2}$$

m_0 and m_1 stand for the mass of the sample before and after immersion, respectively.

Mechanical properties

The PLGA/PLA-blended nanofibrous membranes were cut into several strips with the size of 10 mm $\times$ 50 mm. The thickness of the PLGA/PLA-blended nanofibrous membranes were measured by the digital

fabric thickness gauge [YG(B)141D, Changzhou textile machinery Co., China]. We measured the thickness along the longitudinal direction of the sample. Five points are measured; the average value is the thickness of the sample. The samples were maintained in constant temperature and humidity conditions (T = 25°C, relative humidity = 70%) for 24 h. The tensile properties (breaking strength, elongation, and initial modulus) of the PLGA/PLA nanofibrous scaffolds were measured using an Instron tensile tester (Model 3365, USA). The samples were measured in tension with a crosshead speed of 10 mm/min by the Instron tensile tester. Gauge length was set at 30 mm and a load cell of 100 N was used. Three samples of each material type were tested. Breaking strength and elongation were calculated with eqs. (3) and (4).

$$\text{Breaking strength (MPa)} = \frac{\text{breaking tenacity (N)}}{\text{thickness (mm)} \times \text{width (mm)}} \quad (3)$$

$$\text{Elongation } (\%) = \frac{L_1 - L_0}{L_0} \times 100 \quad (4)$$

L_0 and L_1 stand for the length of sample and the length at break, respectively.

In vitro degradation

The electrospun PLGA/PLA nanofibrous membranes were cut into quadrate samples with the size of 5 cm × 5 cm, and were then immersed in 10 mL of phosphate buffer solution (PBS; pH = 7.4) and hydrolyzed under shaking at 60 rpm at 37°C. After each degradation period (2, 4, 6, 8, and 10 weeks), the samples were washed and dried in a vacuum freeze-dryer for 48 h.

Molecular weight

The electrospun PLGA/PLA-blended nanofibers before and after degradation were dissolved in chloroform. The intrinsic viscosities ([η]) of the PLGA/PLA-blended nanofibers and chloroform solution system were measured with Ubbelohde viscometer (Shanghai Shenyi glasswork Co., China), and the relative molecular weight of electrospun PLGA/PLA nanofibers was determined with eq. (5). Three samples of each material type were tested.

$$\text{Molecular weight} = 1.8404 \times 10^5 \times [\eta]^{1.4939} \quad (5)$$

Weight loss

After each degradation period (2, 4, 6, 8, and 10 weeks), the samples were dried in an oven for 30 min. The weight of PLGA/PLA nanofibrous scaffolds before and after degradation was measured by the analytical balance. The weight loss was calculated with eq. (6). Three samples of each material type were tested.

$$\text{Mass loss } (\%) = \frac{w_0 - w_1}{w_0} \times 100 \quad (6)$$

W_0 and W_1 stand for the mass of the scaffolds before and after degradation, respectively.

Statistical analysis

The data were expressed as (means ± standard deviations; n = 3). Statistical comparisons were performed by SPSS 13.0 and differences were considered as significant when $P < 0.05$.

RESULTS AND DISCUSSION

Morphology and porosity

Figure 1 shows the morphology and diameter's distribution of the PLGA/PLA-blended nanofibers with different blended ratio. As shown in Figure 1(a), the diameter of the pure PLGA nanofibers (PLGA/PLA = 100/0) was fine, and its average diameter was (932 ± 346) nm (Table I). However, the irregular beads (indicated by the rings) could be seen from the SEM image, and the diameter of the fibers was uneven. Fibers' adhesion and bifurcation were also observed in the SEM image. This was probably due to the viscosity of the spinning solution, and only an appropriate viscosity could give rise to the homogeneous, beads-free, and continuous nanofibers.[16,17] Figure 2 shows the viscosity of the PLGA/PLA-blended spinning solution, and the viscosity of the PLGA/PLA (100/0) was relatively low, which induced incomplete solvent evaporation and jet split. As shown in Figure 1(b–d) and Table I, with the decrease of the blended ratios of PLGA to PLA, the diameter of the PLGA/PLA-blended nanofibers increased; however, the irregular beads disappeared, and the distribution of the diameter became more uniformed. This was because the viscosity of the blended spinning solution increased with the decrease of the blended ratio of PLGA to PLA, which improved the spinnability of the spinning solution, and was in favor of the differentiation and stretching of the spraying jet during the electrospinning.

As tissue engineering materials, the scaffolds should have appropriate pore diameter and porosity as it could be in favor of the cell adhesion, proliferation, and growth. Furthermore, the porosity had a greater influence on the mechanical properties of the

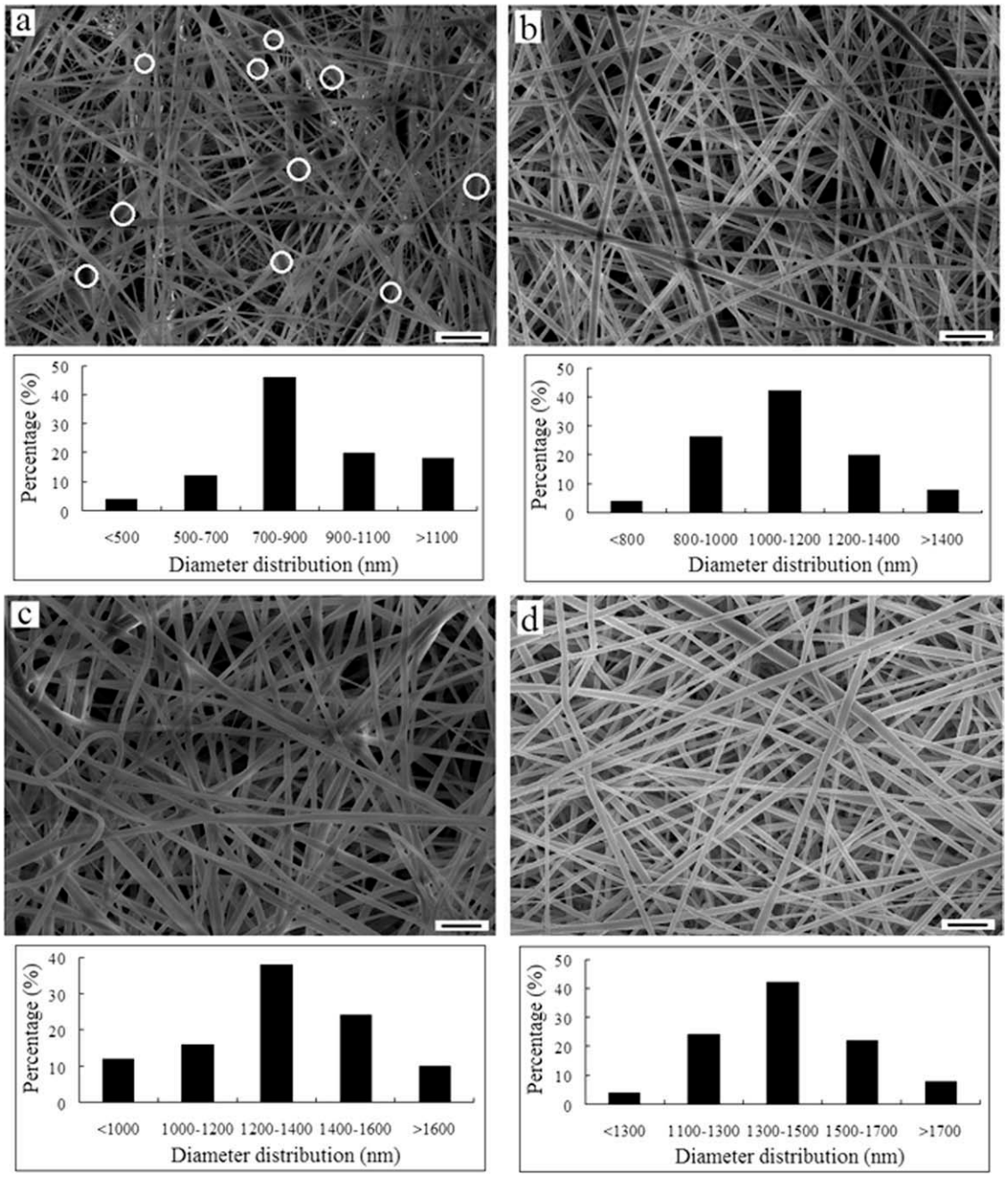

Figure 1 The SEM micrographs and diameter's distribution of the PLGA/PLA-blended nanofibers with different blended ratio: (a) 100/0, (b) 50/50, (c) 30/70, and (d) 0/100 (Scale bar 10 μm).

scaffolds. The pore diameter and porosity of the PLGA/PLA-blended nanofibrous scaffold with different blended ratio were shown in Table I. It could be seen from Table I that the pore diameter increased and porosity decreased respectively with the decrease of the blended ratio of PLGA to PLA.

TABLE I
Morphology and Porosity of the PLGA/PLA Nanofibrous Scaffolds with Different Blended Ratio

Blended ratio	Average diameter (nm)	Thickness (mm)	Bulk density (g/cm^3)	Standard density (g/cm^3)	Pore diameter (nm)	Porosity (%)
100 : 0	932 ± 346	0.48	0.116	1.22	917 ± 324	90.5
50 : 50	1143 ± 292	0.49	0.145	1.24	1098 ± 278	88.3
30 : 70	1346 ± 342	0.50	0.165	1.25	1324 ± 351	86.8
0 : 100	1424 ± 325	0.48	0.185	1.27	1417 ± 316	85.4

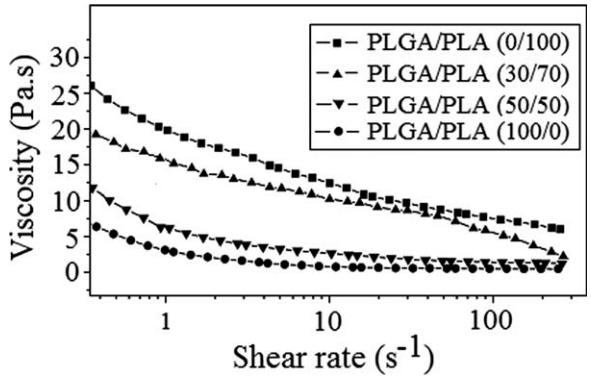

Figure 2 Viscosity of the PLGA/PLA-blended spinning solutions with different blended ratios.

This was due to the fact that average diameter of the PLGA/PLA-blended nanofibers increased with the increase in blended ratio of PLA, which induced the increase of the bulk density, and resulted in the decrease of the porosity. Meanwhile, the range of the nanofibers' interlaced arrangement increased due to the increase of the fibers' diameter, and led to the increase of the pore diameter. It could also be seen from Table I that the porosity of the PLGA/PLA-blended nanofibrous scaffolds ranged from 85 to 90%, which was shown to be desirable for the scaffolds and facilitated the spreading and proliferation of cells, as the preferred porosity of scaffolds used for cellular penetration should generally be within the range of 60–90%.[18–20]

Composition and thermal stability of the PLGA/PLA nanofibers

FTIR analysis

The aim of using FTIR was to characterize the composition of the electrospun PLGA/PLA-blended nanofibers. Figure 3 showed the FTIR spectra of the electrospun PLGA/PLA-blended nanofibers.

As shown in Figure 3, all the four kinds of samples showed similar characteristic absorption peaks at about 1731, 1460, 1385, and 1184 cm^{-1}, which corresponded to the stretching vibration of C=O bonds, and bending vibration of C—H bonds, symmetrical bending vibration of CH_3 bonds and stretching vibration of C—O bonds, respectively. And these bonds were the representative bonds of the PLA and PLGA. However, it could be seen from Figure 3 that the intensity and acuteness of all these characteristic absorption peaks (especially the CH_3 bonds) increased gradually with the increase of the blended ratio of the PLA component. The results indicated that the contents of these bonds increased. This was due to the increase of the blended ratio of the PLA component, as the contents of these bonds were relatively higher in the PLA component.

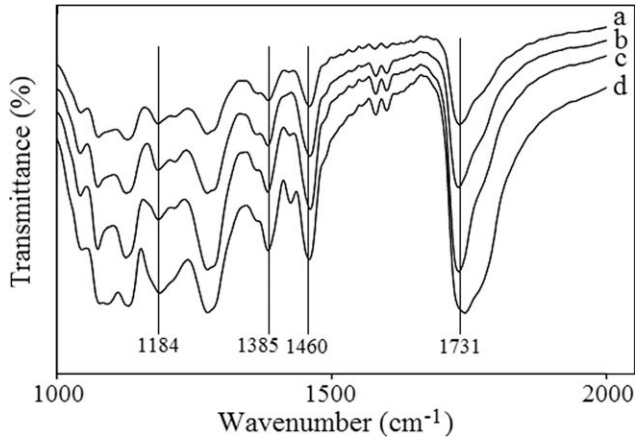

Figure 3 FTIR spectra of the electrospun PLGA/PLA-blended nanofibers with different blended ratio: (a) 100/0, (b) 50/50, (c) 30/70, and (d) 0/100.

Thermal analysis

The structural stability and the crystallinity could be analyzed by thermal analysis. The DSC curves and TG curves of the PLGA/PLA-blended nanofibers with different blended ratio were shown in Figures 4 and 5, respectively. The value of the molten enthalpy (J/g) could respond the crystallinity of the materials.[21] As shown in Figure 4, the pure PLGA nanofibers (PLGA/PLA = 100/0) did not show any molten

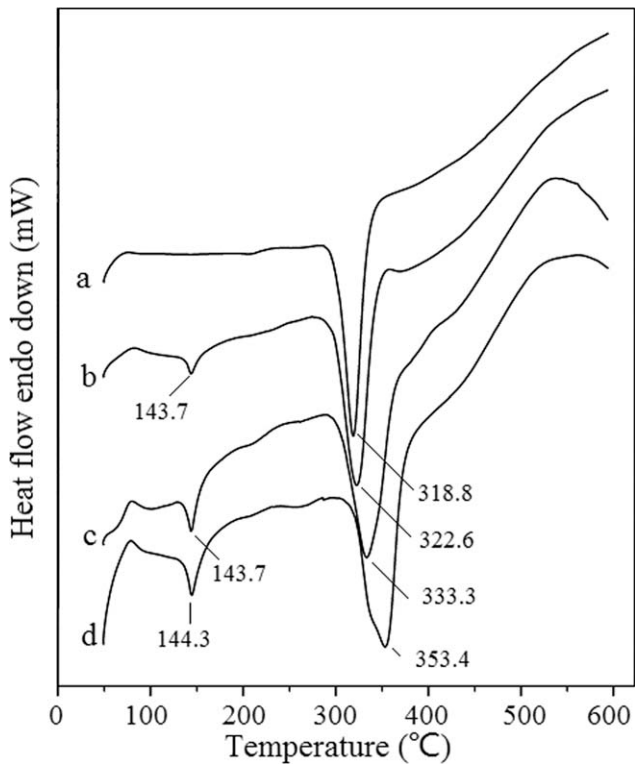

Figure 4 DSC curves of the PLGA/PLA-blended nanofibers with different blended ratio: (a) 100/0, (b) 50/50, (c) 30/70, and (d) 0/100.

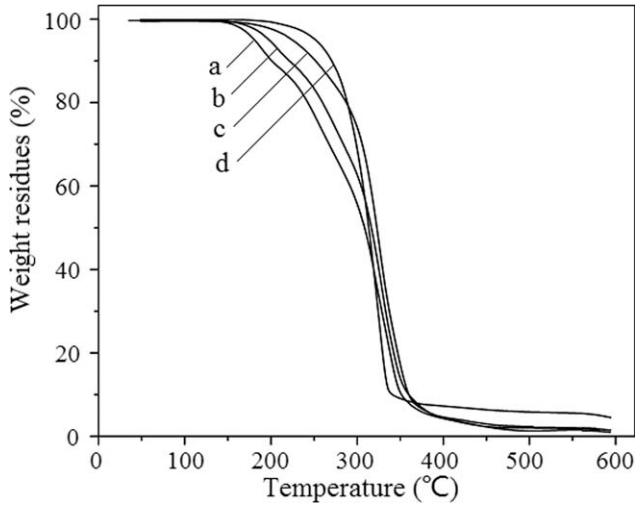

Figure 5 TG curves of the PLGA/PLA-blended nanofibers with different blended ratio: (a) 100/0, (b) 50/50, (c) 30/70, and (d) 0/100.

thermal decomposed peaks, which indicated that the pure electrospun PLGA nanofibers showed noncrystalline structure. With the increase of the blended ratio of the PLA component, the PLGA/PLA-blended nanofibers showed the molten thermal decomposed peaks at 143.7 (50/50), 143.7 (30/70), and 144.3°C (0/100), respectively. The molten thermal decomposed peaks of all the three samples presented at about 150°C, and it was in accord with Ref. [22]. Furthermore, the value of the molten enthalpy (100/0: 0 J/g; 50/50: 16.6 J/g; 30 : 70: 19.7 J/g; 0/100: 21.6 J/g) increased with the increase of blended ratio of the PLA component, which demonstrated that the crystallinity of the PLGA/PLA-blended nanofibers increased with the increase of the blended ratio of the PLA component. It could also be seen from Figure 4 that the maximum thermal decomposition temperature of the PLGA/PLA-blended nanofibers increased with the increase of the blended ratio of the PLA component.

The structural stability of the electrospun PLGA/PLA nanofibers could also be demonstrated by the TG curves. As shown in Figure 5, the thermal decomposed temperature increased with increase of the blended ratio of the PLA component, which indicated that the thermal stability of the PLGA/PLA-blended nanofibers increased gradually with the increase of the blended ratio of the PLA component, and it was keeping with the results of the DSC analysis. All the above results showed that the increase of the PLA component was in favor of the stability of the blended nanofibers. Moreover, we could control the blended ratio of PLGA and PLA to achieve the ideal structural stability and crystallinity.

Wettability of the PLGA/PLA-blended nanofibrous scaffolds

Wettability and hydrophilicity were important properties for biomaterials, which had a great influence on the cell's adhesion, proliferation, and growth.[23–26] The direct expression of the wettability and hydrophilicity of the scaffolds were the water uptake and the CA of a water droplet on the surface. The water uptake and CA of the electrospun PLGA/PLA nanofibrous scaffolds were shown in Figure 6.

The smaller the CA of the scaffold was, the higher hydrophilicity the scaffolds had.[27] As shown in Figure 6(a), the CA of the pure PLGA scaffold (100/0) was 85.8° ± 2.3°. With the increase of the PLA component, the CA of the PLGA/PLA-blended nanofibrous scaffolds was 99.1° ± 1.8° (50/50), 107.6° ± 3.8° (30/70), and 123.4° ± 2.8° (0/100), respectively. The CA of the scaffolds had a significant ($P < 0.05$) increase. The results indicated that the hydrophilicity of the PLGA/PLA-blended nanofibrous scaffolds decreased with the increase of the PLA component. This was due to the fact that there was a large number of methyl present on the molecular chain of LA component, and that the methyl was a high hydrophobic group. Moreover, the GA was a relatively high hydrophilic component. It could be seen from Figure 6(b) that the water uptake of the PLGA/PLA-blended nanofibrous scaffolds decreased remarkably ($P < 0.05$) with the increase of the PLA component, which also demonstrated that the hydrophilicity of the PLGA/PLA-blended nanofibrous scaffolds

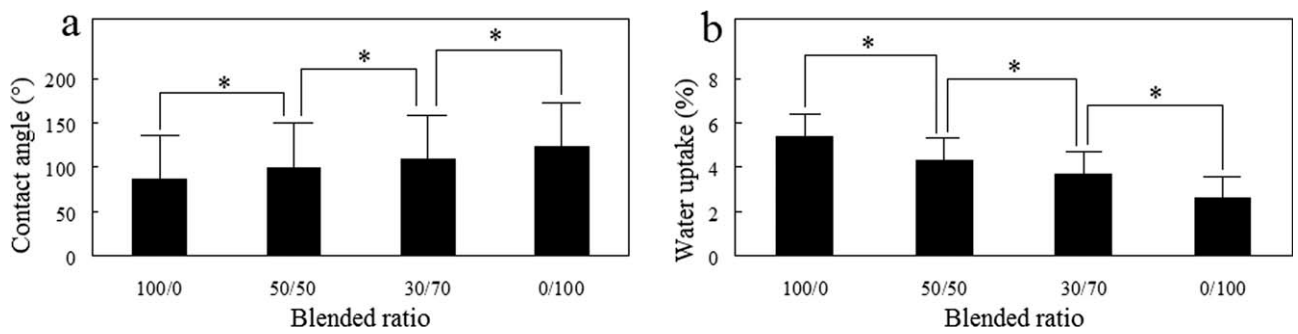

Figure 6 The CA and water uptake of the PLGA/PLA-blended nanofibrous scaffolds with different blended ratio ($P < 0.05$).

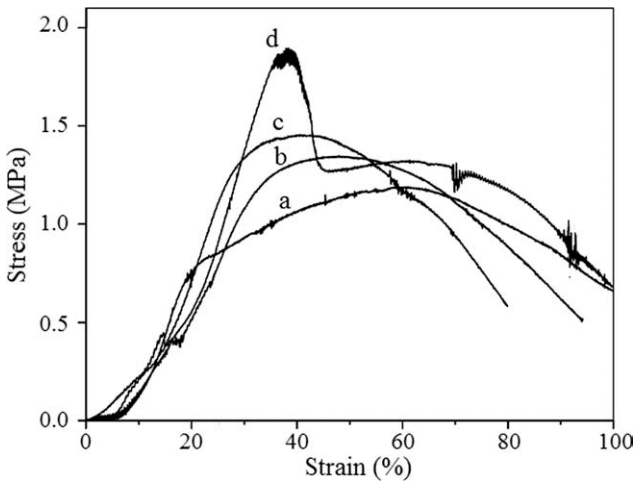

Figure 7 Stress–strain of the PLGA/PLA-blended nanofibrous scaffolds with different blended ratio: (a) 100/0, (b) 50/50, (c) 30/70, and (d) 0/100.

decreased with the increase of the PLA component. The results and analysis were in accord with those of CA. The results indicated that the wettability and hydrophilicity of the PLGA/PLA-blended scaffolds could be controlled by adjusting the blended ratio of PLGA and PLA.

Mechanical properties of the PLGA/PLA-blended nanofibrous scaffolds

As tissue engineering scaffolds, the scaffolds should endure the force from the environment. In this research, we studied the mechanical properties of the PLGA/PLA-blended nanofibrous scaffolds, especially the influence of blended ratio on the mechanical properties. The mechanical properties of the PLGA/PLA-blended nanofibrous scaffolds with different blended ratio (the thickness of the scaffolds was more or less same) were measured. Figure 7 presented the typical stress–strain curves of the electrospun PLGA/PLA-blended nanofibrous scaffolds. Based on the stress–strain curves, breaking strength, elongation at break, and initial modulus of the scaffolds were listed in Table II.

As shown in Figure 7 and Table II, the pure PLGA nanofibrous scaffold showed a relatively lower strength [(1.21 ± 0.03) MPa] and a higher elongation (60.8% ± 2.1%), which showed a flexible characteristic with the initial modulus of (1.99 ± 0.09) MPa. However, the breaking strength and initial modulus increased significantly ($P < 0.05$), and the elongation decreased remarkably ($P < 0.05$). When the blended ratio of the PLGA and PLA was 0/100 (pure PLA), the breaking strength, elongation, and initial modulus of the scaffold were (1.89 ± 0.12) MPa, 38.2% ± 1.9%, and (4.95 ± 0.24) MPa and the initial modulus of the scaffold was almost three times higher than that of the pure PLGA scaffold. The results indicated that the PLGA/PLA-blended scaffolds showed a relatively stiff characteristic with the increase of the PLA component. The remarkable difference of the mechanical properties could be explained from the macroscopic and microcosmic structure of the PLGA/PLA-blended nanofibrous scaffolds. From the macroscopic view, the diameter increased and the porosity decreased with the increase of the PLA component, and this led to the compact arrangement and stable structure of the nanofibers. Therefore, the strength increased and the elongation decreased gradually. From the microcosmic view, the structural stability and the crystallinity increased gradually with the increase of the PLA component, and led to the increase of the scaffold's rigidity. And we could control the blended ratio of PLGA and PLA to achieve the ideal mechanical properties of the PLGA/PLA nanofibrous scaffold according to the demands of the practical application.

In vitro degradation of the PLGA/PLA-blended nanofibrous scaffolds

In vitro degradation study involved analyzing the change in weight loss and molecular weight of the electrospun PLGA/PLA-blended scaffolds during the course of degradation (2, 4, 6, 8, and 10 weeks).

Weight loss

Degradation of the PLGA/PLA-blended nanofibrous scaffolds were expected to cause a decrease in the physical mass of the samples. With the extension of degradation time, partial degradation products dissolved in the PBS solution, and induced the decrease of mass (weight loss). The weight loss could characterize the degradation rate, and a big weight loss meant a high degradation rate. The weight loss of

TABLE II
The Mechanical Properties of the PLGA/PLA Blended Nanofibrous Scaffolds with Different Blended Ratio

Blended ratio	Thickness (mm)	Breaking strength (MPa)	Elongation (%)	Initial modulus (MPa)
100 : 0	0.48	1.21 ± 0.03	60.8 ± 2.1	1.99 ± 0.09
50 : 50	0.49	1.33 ± 0.08	48.4 ± 1.7	2.75 ± 0.16
30 : 70	0.50	1.45 ± 0.03	41.1 ± 1.3	3.53 ± 0.07
100 : 0	0.48	1.89 ± 0.12	38.2 ± 1.9	4.95 ± 0.24

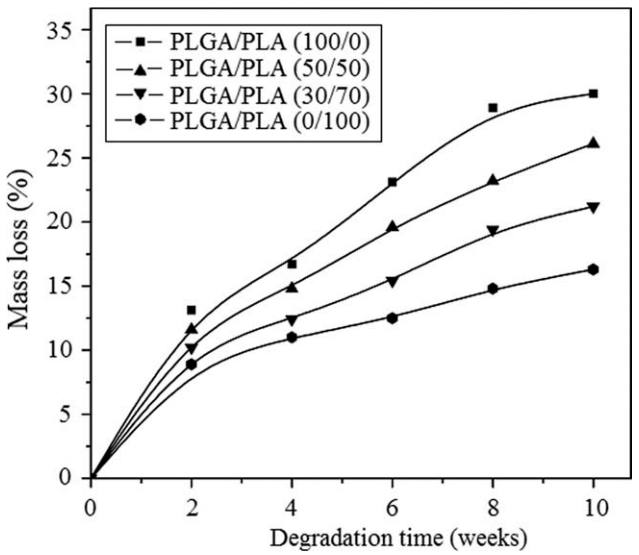

Figure 8 Weight loss of the PLGA/PLA-blended nanofibrous scaffolds during the process of degradation.

the PLGA/PLA-blended nanofibrous scaffolds under different degradation time was shown in Figure 8.

As shown in Figure 8, all the four kinds of PLGA/PLA nanofibrous scaffolds demonstrated a weight loss during the degradation, and with the extension of degradation time, the weight loss of the PLGA/PLA-blended nanofibrous scaffolds increased gradually. The results indicated that all the four kinds of electrospun PLGA/PLA-blended nanofibrous scaffolds were biodegradable polymers. It could also be seen from Figure 8 that the weight loss of the blended nanofibrous scaffolds was different under the same degradation time (2, 4, 6, 8, and 10 weeks), and the PLGA/PLA-blended scaffolds had a higher weight loss with a higher blended ratio of PLGA component. This was because the GA was a relative hydrophilic component, and it could swell quickly in the PBS solution. The PLGA molecular chain ruptured preferentially at the ester bond in the GA-GA or GA-LA, and it resulted in the hydrolyzing of the GA component quickly.[27] Furthermore, as indicated in the thermal analysis section, the crystallinity and structural stability of the PLGA/PLA-blended nanofibers increased with the increase of the blended ratio of the PLA component, so the degradation rate of the PLGA/PLA-blended nanofibrous scaffolds decreased with the increase of the blended ratio of the PLA component. All the above reasons induced that the PLGA/PLA-blended nanofibrous scaffolds had a lower weight loss with a higher blended ratio of PLA component.

Molecular weight

The weight loss study only provided a physical evidence for degradation of the PLGA /PLA nanofibrous scaffolds; however, in order to understand the process at the molecular level, molecular weight of the PLGA/PLA nanofibrous scaffolds was analyzed for the entire duration of the degradation. The change of the molecular weight in the process of the degradation was shown in Figure 9.

As shown in Figure 9, the molecular weight of all the PLGA/PLA-blended nanofibrous scaffolds with different blended ratio decreased gradually with the extension of degradation time. This was due to the fact that the macromolecules were cut off by water molecule during the degradation, which induced that the molecular weight and intermolecular force of the PLGA/PLA-blended nanofibers decreased. The results also indicated that all the four kinds of electrospun PLGA/PLA-blended nanofibrous scaffolds were biodegradable polymers. It could also be seen from Figure 9 that the degradation rate of the PLGA/PLA-blended nanofibrous scaffolds increased with the increase of the blended ratio of the PLGA component. The results and reasons were keeping with those of the weight loss section. Furthermore, as shown in Figure 9, all the four kinds of samples showed a higher degradation rate during the first 2 weeks of degradation, and the degradation rate trended to be gentle after 2 weeks. This was because that the degradation first occurred in the amorphous region of the blended nanofibers, and then occurred in the crystalline region.[28,29] The molecular chains' arrangement of the amorphous region was random and incompact, which induced that it was easy to degrade. However, the molecular chains' arrangement of the crystalline region was regular and compact, which was difficult to degrade. Thus, the blended samples showed a higher degradation rate

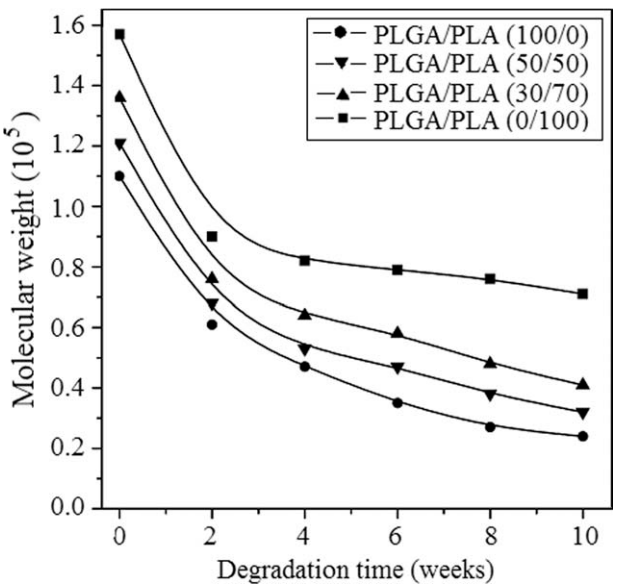

Figure 9 Molecular weight of the PLGA/PLA-blended nanofibrous scaffolds during the process of degradation.

during the first 2 weeks of degradation and a lower degradation rate after 2 weeks of degradation.

CONCLUSION

In the present study, the PLGA/PLA-blended nanofibrous scaffolds were prepared by electrospinning for potential use in tissue engineering scaffolds. The electrospun PLGA/PLA-blended nanofibrous scaffolds possessed nanofibrous and porous structure with average diameter from 900 to 1500 nm and porosity from 85 to 90%. The structural stability, crystallinity, wettability, and mechanical properties of the electrospun PLGA/PLA-blended nanofibrous could be controlled by regulating the blended ratio of the PLGA and PLA. The electrospun PLGA/PLA nanofibrous scaffolds could biodegrade gradually with the extension of degradation time, and the degradation rate could also be regulated by adjusting the blended ratio of the PLGA and PLA. And all the investigations demonstrated that the electrospun PLGA/PLA nanofibrous scaffolds were appropriate candidates for tissue engineering materials.

The authors are indebted to the Testing Center of Soochow University for experimental support.

References

1. Matthews, J. A.; Wnek, G. E.; Simpson, D. G.; Bowlin, G. L. Biomacromolecules 2002, 3, 232.
2. Han, J.; Zhang, J. F.; Yin, R. X.; Ma, G. P.; Yang, D. Z.; Nie, J. Carbohydr Polym 2011, 83, 270.
3. Wang, S. D.; Zhang, Y. Z.; Yin, G. B.; Wang, H. W.; Dong, Z. H. Mater Sci Eng C 2010, 30, 670.
4. Sun, K.; Li, Z. H. eXPRESS Polym Lett 2011, 5, 342.
5. Wang, S. D.; Zhang, Y. Z.; Wang, H. W.; Dong, Z. H. Int J Biol Macromol 2011, 48, 345.
6. Anderson, J. M.; Shive, M. S. Adv Drug Deliv Rev 1997, 28, 5.
7. Zhang, H.; Cui, W.; Bei, J.; Wang, S. Polym Degrad Stab 2006, 91, 1929.
8. Shin, H. J.; Lee, C. H.; Cho, I. H.; Kim, Y. J.; Lee, Y. J.; Kim, I. A. J Biomater Sci Polym Ed 2006, 17, 103.
9. You, Y.; Youk, J. H.; Lee, S. W.; Min, B. M.; Lee, S. J.; Park, W. H. Mater Lett 2006, 60, 756.
10. Liu, S. J.; Kau, Y. C.; Chou, C. Y.; Chen, J. K.; Wu, R. C.; Yeh, W. L. J Membr Sci 2010, 355, 53.
11. Meng, Z. X.; Wang, Y. S.; Ma, C.; Zheng, W.; Li, L.; Zheng, Y. F. Mater Sci Eng C 2010, 30, 1204.
12. Stevanovic, M.; Pavlovic, V.; Petkovic, J.; Filipic, M.; Uskokovic, D. eXPRESS Polym Lett 2011, 5, 996.
13. Rajesh, V.; Kirubanandan, S.; Dhirendra, S. K. Polym Degrad Stab 2010, 95, 1605.
14. Yin, G. B.; Zhang, Y. Z.; Wang, S. D.; Shi, D. B.; Dong, Z. H.; Fu, W. G. J Biomed Mater Res A 2010, 93, 158.
15. Vaz, C. M.; Tuij, S. V.; Bouten, C. V. C. Acta Biomater 2005, 1, 575.
16. Zhang, F.; Zuo, B.; Zhang, H.; Bai, L. Polymer 2009, 50, 279.
17. Bao, W.; Zhang, Y.; Yin, G.; Wu, J. e-Polymers 2008, 98, 1.
18. Courtney, T.; Sacks, M. S.; Stankus, J.; Guan, J.; Wagner, W. R. Biomaterials 2006, 27, 3631.
19. Yin, G. B.; Zhang, Y. Z.; Bao, W. W.; Wu, J. L.; Shi, D. B.; Dong, Z. H.; Fu, W. G. J Appl Polym Sci 2009, 111, 1471.
20. Wang, S. D.; Zhang, Y. Z.; Yin, G. B.; Wang, H. W.; Dong, Z. H. J Appl Polym Sci 2009, 113, 2675.
21. Wang, S. D.; Li, S. Y.; Zhang, Y. Z.; Wang, H. W. Tech Textil China 2009, 27, 8.
22. Schmack, G.; Aquino, E.; Vqoel, R. Chem Fibers Int 2005, 55, 292.
23. Cui, W. G.; Zhu, X. L.; Yang, Y.; Li, X. H.; Jin, Y. Mater Sci Eng C 2009, 29, 1869.
24. Zheng, J. F.; He, A. H.; Li, J. X.; Xu, J.; Han, C. C. Polymer 2006, 47, 7095.
25. Cui, W. G.; Li, X. H.; Zhou, S. B.; Weng, J. Polym Degrad Stab 2008, 93, 731.
26. Nirmala, R.; Park, H. M.; Navamathavan, R.; Kang, H. S.; El-Newehy, M. H.; Kim, H. Y. Mater Sci Eng C 2011, 31, 486.
27. Lu, L.; Peter, S. J.; Lyman, M. D.; Lai, H. L.; Leite, S. M.; Tamada, J. A.; Uyama, S.; Vacanti, J. P.; Langer, R.; Mikos, A. G. Biomaterials 2000, 21, 1837.
28. Huang, M. H.; Li, S. M.; Vert, M. Polymer 2004, 45, 8675.
29. Stefani, M.; Coudane, J.; Vert, M. Polym Degrad Stab 2006, 91, 2554.